

4. R. M. Sanderson, *Meteorol. Mag.* **104**, 313 (1975).
5. V. F. Zakharov, *Technical Document WMO/TD 782* (World Meteorological Organization, Geneva, 1997) [translation from *Morskije l'dy v klimaticheskoi sisteme* (Sea ice in the climate system) (Gidrometeoizdat, St. Petersburg, 1996)].
6. J. E. Walsh and C. M. Johnson, *J. Phys. Oceanogr.* **9**, 580 (1979).
7. K. Y. Vinnikov et al., *Sov. Meteorol. Hydrol.* **6**, 1 (1980).
8. C. F. Ropelewski, *Adv. Space Res.* **5**, 275 (1985).
9. G. Kukla and J. Gavin, *Science* **214**, 497 (1981).
10. P. Gloersen and W. J. Campbell, *J. Geophys. Res.* **93**, 10666 (1988).
11. C. L. Parkinson and D. J. Cavalieri, *J. Geophys. Res.* **94**, 14499 (1989).
12. P. Gloersen et al., *NASA Spec. Publ. SP-511*, 1 (1992).
13. W. L. Chapman and J. E. Walsh, *Bull. Am. Meteorol. Soc.* **74**, 33 (1993).
14. E. Bjorgo, O. M. Johannessen, M. W. Niles, *Geophys. Res. Lett.* **24**, 413 (1997).
15. D. J. Cavalieri, P. Gloersen, C. L. Parkinson, J. C. Comiso, H. J. Zwally, *Science* **278**, 1104 (1997).
16. C. L. Parkinson, D. J. Cavalieri, P. Gloersen, H. J. Zwally, J. C. Comiso, *J. Geophys. Res.* **104**, 20837 (1999).
17. D. J. Cavalieri, C. L. Parkinson, P. Gloersen, J. C. Comiso, H. J. Zwally, *J. Geophys. Res.* **104**, 15803 (1999).
18. S. Manabe, R. J. Stouffer, M. J. Spelman, K. Bryan, *J. Clim.* **4**, 785 (1991).
19. S. Manabe and R. J. Stouffer, *Bull. Am. Meteorol. Soc.* **78**, 1177 (1997).
20. J. Haywood et al., *Geophys. Res. Lett.* **24**, 1335 (1997).
21. D. A. Rothrock, Y. Yu, G. A. Maykut, *Geophys. Res. Lett.*, in press.
22. T. C. Johns et al., *Clim. Dyn.* **13**, 103 (1997).
23. R. J. Stouffer, S. Manabe, K. Y. Vinnikov, *Nature* **367**, 634 (1994).
24. Battisti et al. [D. S. Battisti, C. M. Bitz, R. E. Moritz, *J. Clim.* **10**, 1909 (1997)], using a more complex sea ice model, with explicit snow cover and multiple ice layers, claim that the sea ice model used here underestimates the low-frequency variability of the sea ice thickness. Their model produces a longer time scale of response, resulting in larger low-frequency variability of sea ice, and they

claim that it is more realistic. Furthermore, they postulate that the sea ice response to changes in the radiative forcing would be too fast with our simple model. But, they admit that observations are not good enough to distinguish between the high variability of ice they calculate and the lower GFDL variability, and their model is only of ice thickness, not extent, and ignores any spatial heterogeneity. Our findings in this report, which compare the model results to the observations, contradict their conclusions, at least for sea ice extent in the NH. The modeled variability of the sea ice extent agrees quite well with the detrended observations, and the response to increasing greenhouse gases also seems realistic.

25. We thank S. Manabe, J. Mahlman, I. Held, M. Winton, K. W. Dixon, and T. Broccoli for very useful discussions on the work and suggestions on the manuscript; W. Chapman, C. Ropelewski, E. Bjorgo, and O. M. Johannessen for supplying us with observed sea ice extent data; and C. Coughlan for assistance in work with the Hadley Centre model output. This work was supported by joint NOAA and U.S. Department of Energy grants NA66GPO438 and NA96GPO117 and by the NASA Polar Programs Office.

18 August 1999; accepted 25 October 1999

Satellite Evidence for an Arctic Sea Ice Cover in Transformation

Ola M. Johannessen,^{1,2*} Elena V. Shalina,³ Martin W. Miles^{1,4}

Recent research using microwave satellite remote sensing data has established that there has been a reduction of about 3 percent per decade in the areal extent of the Arctic sea ice cover since 1978, although it is unknown whether the nature of the perennial ice pack has changed. These data were used to quantify changes in the ice cover's composition, revealing a substantial reduction of about 14 percent in the area of multiyear ice in winter during the period from 1978 to 1998. There also appears to be a strong correlation between the area of multiyear ice and the spatially averaged thickness of the perennial ice pack, which suggests that the satellite-derived areal decreases represent substantial rather than only peripheral changes. If this apparent transformation continues, it may lead to a markedly different ice regime in the Arctic, altering heat and mass exchanges as well as ocean stratification.

Enhanced Arctic warming and a retreating sea ice cover are common features in modeled climate change scenarios (1, 2). Quantitative observational evidence for changes in the sea ice cover may be obtained from satellite-borne sensors measuring low-frequency microwave (millimeter to meter wavelength) radiation. Microwave-derived sea ice time series are now among the longest continuous satellite-derived geophysical records, extending over two decades. The Nimbus-7 Scanning Multichannel Microwave Radiometer (SMMR) provided data from 1978 to 1987, and the follow-up Special Sensor Microwave/Imagers (SSM/I)

onboard Defense Meteorological Satellite Program (DMSP) satellites F8, F11, and F13 have provided data since 1987. The multifrequency brightness temperature (T_B) data are used to calculate total ice concentration (the percent of ice-covered ocean), from which total ice area (the area of ice-covered ocean) and total ice extent (the area within the ice-ocean margin) are derived. Analyses of SMMR and SSM/I data have detected a reduction of about 3% per decade in total ice area (3, 4) and extent (3–5) in the Arctic since 1978. The observed decreases are due largely to reduced summer ice extent in the Eurasian Arctic in the 1990s, with record low arctic ice minima observed in 1990, 1993, and 1995, linked to regional atmospheric circulation anomalies (6). The reduced summer ice extent implies a consequential transformation of the winter ice cover toward thinner seasonal ice. There have been fragmentary indications of unusual conditions in recent years [such as reduced ice concentration in the Siberian sector of the perennial ice pack in the 1990s (6) and reduced ice thickness in parts of the Arctic

since the 1970s, based on submarine sonar data (7)]. However, it has remained unknown whether the nature of the perennial ice pack as a whole has changed. Perennial multiyear (MY) ice (ice that has survived the summer melt) is about three times thicker than seasonal or first-year (FY) ice (~1 to 2 m), so that changes in ice type distribution could both reflect and effect climate change.

Because MY ice, FY ice, and open water have different radiative properties, algorithms applied to multichannel microwave data can separate each of these surface components, at least in winter when the signatures are relatively stable (8–11). The possibility of monitoring interannual variations in MY ice area with satellite microwave data has been explored (8, 9) but remains unrealized. We produced and analyzed spatially integrated time series of MY and FY ice areas in winter derived from SMMR and SSM/I data from 1978 to 1998, revealing the ice cover's changing composition.

In general, combined SMMR-SSM/I time series are produced at the geophysical parameter level rather than the sensor radiance or T_B level. The methods used here are based on the approach we used previously (4) for merging SMMR-SSM/I sea ice time series, with additional methods used for robust estimation of MY and FY ice areas. Briefly, the NORSEX (11, 12) algorithm is used to calculate ice concentration from SMMR (18 and 37 GHz) and SSM/I (19 and 37 GHz) T_B data, with the SMMR T_B s adjusted for slight sensor drift (3, 4). Total ice concentration, area, and extent are iteratively calculated and adjusted (4) for the SMMR-SSM/I overlap period (July to August 1987) to less than 1% difference for all parameters. No adjustments are made to the F8, F11, and F13 SSM/I T_B s because (i) the individual sensor drifts are negligible (13); (ii) relative SSM/I T_B inter-calibrations are not advantageous (14); and (iii) biases are not significant for hemispheric sea ice parameters, notwith-

¹Nansen Environmental and Remote Sensing Center, Edvard Griegsvai 3a, 5059 Bergen, Norway. ²Geophysical Institute, University of Bergen, 5007 Bergen, Norway. ³Nansen International Environmental and Remote Sensing Center, Korpusnaya ulitsa 18, 197110 St. Petersburg, Russia. ⁴Department of Geography, University of Bergen, Breiviksveien 40, 5045 Bergen, Norway.

*To whom correspondence should be addressed. E-mail: Ola.Johannessen@nrsc.no

standing some regional differences (14).

The algorithm is sensitive to the frequency-dependent surface emissivity (ϵ) of the three surfaces (MY ice, FY ice, and open water), in such a way that its proper specification is essential for accurate separation (9–12). The MY ice analysis is restricted to the five winter months (November through March) when ϵ_{MY} is relatively stable as compared to the rest of the year. Because the SMMR-SSM/I sensor overlap occurred during the boreal summer (a time of unstable ice signatures), it is unreasonable to directly intercalibrate the SMMR- and SSM/I-derived MY and FY ice areas, as was done for total ice concentration (4). Instead, the estimates were made by (i) fine-tuning ϵ_{MY} at 18 GHz (SMMR) and 19 GHz (SSM/I), based on arctic field measurements (10, 11); (ii) fine-tuning the weather filters to reduce false ice signatures off the main ice edge (15); (iii) analyzing spatio-temporal variations in the MY ice distribution for coherence; and (iv) analyzing each summer's minimum ice area in conjunction with the following winter's MY ice area—these two values should correspond (8).

Procedure (iv) confirmed a close correspondence (correlation coefficient $r \sim 0.82$, $P < 0.01$), with the winter-averaged MY ice area being only 13% less than the summer minimum; this is much closer than the 25 to 40% obtained previously (8). The difference is partially explained by the metamorphosis of second-year ice into mature MY ice (8, 9), so that the microwave-derived MY ice area generally increases during the winter (Fig. 1)—the MY ice area in late winter (March) is only 9% less than the summer minimum. The remaining difference may be explained largely by substantive losses from ice outflow through the Fram Strait and East Greenland Current from September to March (16). Therefore, we consider our time series of MY and FY ice areas to be geophysically sound representations of the character of the winter ice cover through the observation period.

Figure 1 shows the variability of microwave-derived MY ice area in the Arctic in winter 1978–98. The winter-averaged MY area decreased $0.031 \times 10^6 \text{ km}^2 \text{ year}^{-1}$, as compared with a total ice area decrease of $0.024 \times 10^6 \text{ km}^2 \text{ year}^{-1}$ averaged over the same 5 months. The difference ($0.007 \times 10^6 \text{ km}^2 \text{ year}^{-1}$) represents replacement by FY ice, so that the proportion of MY ice to FY ice changed accordingly. The $0.031 \times 10^6 \text{ km}^2 \text{ year}^{-1}$ negative trend in MY ice area is statistically significant at $P \sim 0.04$ and represents a decrease of $\sim 7\%$ per decade (a 14% reduction from 1978–98), as compared to a decrease in the total ice area in winter of $\sim 2\%$ per decade.

Our results showing this 14% reduction in MY ice area in the past two decades are corroborated by other analyses. First, the winter MY ice areas correspond closely to the preceding summer minima, which other analyses have

found to be decreasing most in recent years (6). Second, an analysis of SMMR and SSM/I data found an 8% increase (5.3 days) in the length of the sea ice melt season in the Arctic from 1978 to 1996 (17). Third, independent data from oceanographic field observations have revealed changes in upper ocean water masses (18) between 1975 and 1997 that are assumed to stem from a substantial melting of perennial MY ice.

In order to evaluate the importance of the reductions in MY ice area in terms of the ice cover's mass balance, spatially and temporally coincident data on ice thickness are needed. Although there are no data sets covering the entire Arctic, near-coincident transects of submarine sonar data have revealed a decrease in ice thickness in the Eurasian Basin since at least the 1970s (7, 19). Moreover, spatially averaged basin-wide or regional ice thickness estimates have been made with the use of surface elastic-

gravity wave measurements from around Russian *North Pole* drifting stations (20, 21). Measurements of ice surface oscillations were carried out regularly in the eastern Arctic Ocean from 1972 to 1991. Elastic gravity waves in ice are caused by ocean swell waves generated in ice-free oceans, strong wind zones, and ridging processes. The long waves (200 to 500 m) propagate for hundreds to thousands of kilometers with weak dampening. Long wave propagation is not disturbed by heterogeneous ice conditions such as hummocks, thin ice, and open leads, which have a relatively small horizontal dimension as compared to wavelength.

The measured surface oscillation parameters (wavelength, wave period, and direction) are related to ice thickness through a dispersion relation, given the elastic property of the sea ice. Directional ice thickness estimates can be de-

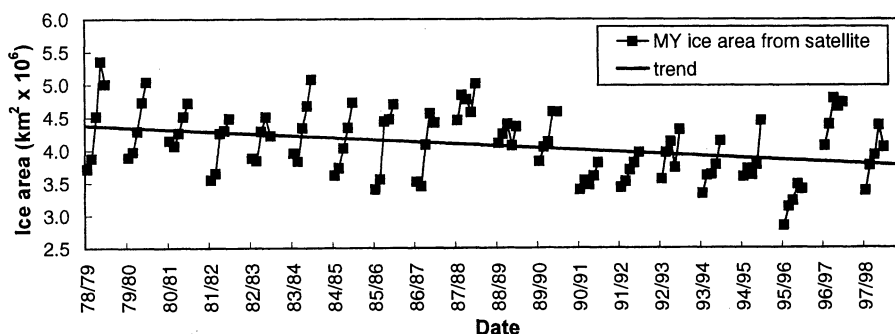


Fig. 1. Arctic MY sea ice area in winter 1978–98, as derived from satellite passive microwave sensor data. The image data are multifrequency multipolarization T_b s measured by SMMR from 1978 to 1987 and by the DMSP SSM/I from 1987 to 1998. The SMMR data were acquired at 2-day intervals and consist of polarized T_b s measured at about 7, 11, 18, 21, and 37 GHz, horizontally and vertically polarized. The SSM/I data are 1-day polarized T_b s measured at about 19, 22, 37, and 85 GHz. The data sets are issued by the National Snow and Ice Data Center in Boulder, Colorado. The T_b s depend on the particular concentration of open water, FY ice, and MY ice within each 25-by-25-km image pixel. The NORSEX ice concentration algorithm (11, 12) is used to separate these components and calculate their respective areas. The linear regression reveals that the microwave-derived MY ice area decreased by $\sim 610,000 \text{ km}^2$ during the 20-year period, representing an $\sim 14\%$ decrease.

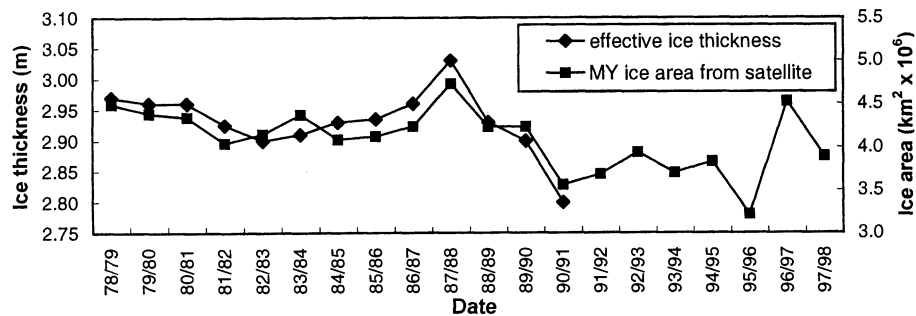


Fig. 2. Arctic Ocean sea ice thickness and MY sea ice area in winter, as derived from surface measurements (1978–91) and satellite passive microwave sensor data (1978–98), respectively. The area-averaged ice thickness estimates are based on surface-based measurements of ice surface oscillations made from the Russian *North Pole* drifting stations in the perennial ice pack of the eastern Arctic Ocean (20, 21). The methods used to estimate MY ice area are described in the text. The high correlation ($r \sim 0.88$) between the two ice parameters during the overlap period suggests that (i) the observed areal decrease in MY ice is associated with a volumetric decrease in the total sea ice cover in winter and (ii) the average ice thickness has continued to vary with MY ice area after the surface measurements ended in 1991.

rived with the wave algorithm with an error of less than 10% if an averaged elastic property of the sea ice is used (20). The wave propagation characteristics result in a natural averaging of the ice thicknesses. Further, by averaging the directional ice thicknesses, a spatially averaged effective ice thickness is obtained (20, 21). Here we compare these ice thickness estimates (21) to MY ice area during the common observation period. Figure 2 shows the interannual variability of the mean end-of-winter (April–May) ice thickness and winter MY ice area from 1978/79 to 1990/91. The decreases are more pronounced from 1987 onward, associated with changes in atmospheric circulation (such as an increase in the frequency of low-pressure systems in the Arctic) since the late 1980s (6). The high degree of correspondence ($r \sim 0.88$, $P < 0.01$) between these independent data (which was unexpected; after all, MY ice can become substantially thinner and still count toward the MY ice area) reveals that a relationship exists between ice thickness and area. The potential importance of this observation is twofold. First, it indicates that the observed decrease in MY ice area from 1978 to 1998 represents a substantial (that is, a negative mass balance) rather than peripheral effect. Second, it suggests that the interannual variability and trends of arctic ice thickness may be estimated to a first order through an empirical relationship with MY ice area, as 77% (r^2) of the variability in ice thickness is explained by variability in MY ice area, the more readily monitored parameter. However, this relationship requires further investigation, and it is noted that the changes in effective ice thickness (21) are considerably less than those reported elsewhere (19).

The balance of evidence thus indicates an ice cover in transition, which, if continued, could lead to a markedly different ice-ocean-atmosphere regime in the Arctic. However, 20 years are inadequate to establish that this is a long-term trend rather than reflecting decadal-scale atmosphere-ocean variability such as the North Atlantic Oscillation (NAO) (22). The NAO is known to be strongly coupled to regional sea ice fluctuations (15, 23), and here we find its winter index (22) to be lag-correlated with the following summer minimum ice area and hence the following winter MY ice area (both $r \sim -0.54$, $P \sim 0.02$). Thus the NAO index explains $\sim 25\%$ (r^2) of the MY ice variability.

Further satellite monitoring and analysis of the sea ice cover, together with oceanographic and atmospheric data, are needed to better understand the patterns and processes behind these changes. Moreover, because sea ice parameters are hemispherically integrated measurements, we recommend that quantitative comparisons be made with ice cover output from global coupled climate models in the same manner as global average atmo-

spheric temperature observations, for improved assessment and prediction of global warming in the polar regions.

References and Notes

1. S. Manabe, M. J. Spelman, R. J. Stouffer, *J. Clim.* **5**, 105 (1992).
2. J. F. B. Mitchell, T. C. Johns, J. M. Gregory, S. F. B. Tett, *Nature* **376**, 501 (1995).
3. O. M. Johannessen, M. W. Miles, E. Bjørge, *Nature* **376**, 126 (1995).
4. E. Bjørge, O. M. Johannessen, M. W. Miles, *Geophys. Res. Lett.* **24**, 413 (1997).
5. D. J. Cavalieri, P. Gloersen, C. L. Parkinson, H. J. Zwally, J. C. Comiso, *Science* **278**, 1104 (1997).
6. J. Maslanik, M. C. Serreze, R. G. Barry, *Geophys. Res. Lett.* **23**, 1677 (1996). A comprehensive spatiotemporal analysis of satellite data from 1978 to 1996 revealed some of the greatest decreases ($>20\%$) to be in the summer ice cover over large parts of the East Siberian and Kara seas [C. L. Parkinson, D. J. Cavalieri, P. Gloersen, H. J. Zwally, J. C. Comiso, *J. Geophys. Res.* **104**, 20,837 (1999)].
7. P. Wadhams, *Nature* **345**, 795 (1990). Analysis of data on sea ice thickness from the Greenland Sea and Eurasian Basin acquired from British submarine cruises in 1976 and 1987 showed a 15% decrease. However, the requisite data sets from submarine transects needed to reliably test for changes in overall arctic ice thickness have remained unavailable [P. Wadhams, *J. Geophys. Res.* **102**, 27951 (1997)], although progress is being made; see (19). Additionally, methods of estimating spatially integrated sea ice thickness using spaceborne altimetry appear promising [N. R. Peacock *et al.*, in *Proceedings of the International Geosciences and Remote Sensing Symposium*, Seattle, WA, 6 to 10 July 1998, T. I. Stein, Ed. (IEEE, Piscataway, NJ, 1998), pp. 1964–1966] and may be applied to continuous satellite altimeter data sets made since 1991.
8. J. C. Comiso, *J. Geophys. Res.* **95**, 13,411 (1990).
9. P. Gloersen *et al.*, *Arctic and Antarctic Sea Ice: 1978–1987: Satellite Passive Microwave Observations and Analysis* (NASA, Washington, DC, 1992).
10. T. Grenfell, *J. Geophys. Res.* **97**, 3485 (1992).
11. NORSEX Group, *Science* **220**, 781 (1983).
12. E. Svendsen *et al.*, *J. Geophys. Res.* **88**, 2781 (1983).
13. D. J. Cavalieri, C. L. Parkinson, P. Gloersen, J. C. Comiso, H. J. Zwally, *J. Geophys. Res.* **104**, 15,803 (1999).
14. J. Stroeve, X. Li, J. Maslanik, *Remote Sens. Environ.* **64**, 132 (1998).
15. P. Gloersen and D. J. Cavalieri, *J. Geophys. Res.* **91**, 3913 (1986).
16. R. Kwok and D. A. Rothrock, *J. Geophys. Res.* **104**, 5177 (1999).
17. D. M. Smith, *Geophys. Res. Lett.* **25**, 655 (1998).
18. M. G. McPhee, T. P. Stanton, J. H. Morison, D. G. Martinson, *Geophys. Res. Lett.* **25**, 1729 (1998).
19. D. A. Rothrock, Y. Yu, and G. A. Maykut (*Geophys. Res. Lett.*, in press) compared sea ice draft data acquired by the Scientific Ice Expeditions (SCICEX) program in the mid-1990s with data from 1958 and 1976, finding a mean decrease of 1.3 m (around 40%) in ice thickness over the deep Arctic Ocean, with greater decreases in the eastern and central Arctic than in the western Arctic. These trends are much greater than the ~ 0.1 m reported in (21) and shown in our Fig. 2, although the data sets are not directly comparable. First, the effective ice thickness estimates in Fig. 2 are from 1978–91, so that there is no overlap. Second, the data are from different seasons, and summer and winter trends are not expected a priori to be similar. Third, the 1990s data analyzed by Rothrock *et al.* are from 1993–97, which happens to be a period of unusually large reductions in the summer ice cover, especially in the eastern Arctic, with record low ice minima in 1993 and 1995 (6).
20. A. P. Nagurnyi, V. G. Korostelev, P. A. Abaza, *Bull. Russian Acad. Sci. Phys. Suppl. Phys. Vib.* **58**, 168 (1994).
21. A. P. Nagurnyi, V. G. Korostelev, V. V. Ivanov, *Meteorol. Hydrol.* **3**, 72, (1999) (Russian; English translation available from the Nansen Environmental and Remote Sensing Center).
22. J. W. Hurrell, *Science* **269**, 676 (1995).
23. L. A. Mysak and S. A. Venegas, *Geophys. Res. Lett.* **25**, 3607 (1998).
24. Supported by grants from the European Union's program International Association for the Promotion of Co-operation with Scientists from the Independent States of the Former Soviet Union (INTAS), the Norwegian Research Council's programs International Co-operation: Central and Eastern Europe and Arctic Radiation and Heat, and the Norwegian Space Centre. The satellite data were provided by the National Snow and Ice Data Center in Boulder, CO. We thank A. P. Nagurnyi and H. Sagen for useful discussions on ice thickness retrieval and the two anonymous reviewers for useful comments on the manuscript.

11 August 1999; accepted 27 October 1999

Domain Movement in Gelsolin: A Calcium-Activated Switch

Robert C. Robinson,¹ Marisan Mejillano,² Vincent P. Le,¹ Leslie D. Burtnick,³ Helen L. Yin,² Senyon Choe^{1*}

The actin-binding protein gelsolin is involved in remodeling the actin cytoskeleton during growth-factor signaling, apoptosis, cytokinesis, and cell movement. Calcium-activated gelsolin severs and caps actin filaments. The 3.4 angstrom x-ray structure of the carboxyl-terminal half of gelsolin (G4–G6) in complex with actin reveals the basis for gelsolin activation. Calcium binding induces a conformational rearrangement in which domain G6 is flipped over and translated by about 40 angstroms relative to G4 and G5. The structural reorganization tears apart the continuous β sheet core of G4 and G6. This exposes the actin-binding site on G4, enabling severing and capping of actin filaments to proceed.

The cellular actin scaffold is continuously reorganized in response to a variety of signals. Apoptosis promotes dismantling of the actin cytoskeleton, and growth factor stimulation induces actin filament assembly at the plasma membrane, which leads to cell shape changes and movement. Gelsolin is a calci-

um-activated regulator of these cytoskeletal and motile functions of actin (1). Elevated calcium concentrations activate the filament severing and capping activities of gelsolin, which results in more actin filaments with a shorter average length. The six domains of gelsolin, G1–G6, probably arose through a

LINKED CITATIONS

- Page 1 of 1 -



You have printed the following article:

Satellite Evidence for an Arctic Sea Ice Cover in Transformation

Ola M. Johannessen; Elena V. Shalina; Martin W. Miles

Science, New Series, Vol. 286, No. 5446. (Dec. 3, 1999), pp. 1937-1939.

Stable URL:

<http://links.jstor.org/sici?sici=0036-8075%2819991203%293%3A286%3A5446%3C1937%3ASEFAAS%3E2.0.CO%3B2-R>

This article references the following linked citations:

References and Notes

⁵ **Observed Hemispheric Asymmetry in Global Sea Ice Changes**

D. J. Cavalieri; P. Gloersen; C. L. Parkinson; J. C. Comiso; H. J. Zwally

Science, New Series, Vol. 278, No. 5340. (Nov. 7, 1997), pp. 1104-1106.

Stable URL:

<http://links.jstor.org/sici?sici=0036-8075%2819971107%293%3A278%3A5340%3C1104%3AOHAIGS%3E2.0.CO%3B2-1>

¹¹ **Norwegian Remote Sensing Experiment in a Marginal Ice Zone**

NORSEX Group

Science, New Series, Vol. 220, No. 4599. (May 20, 1983), pp. 781-787.

Stable URL:

<http://links.jstor.org/sici?sici=0036-8075%2819830520%293%3A220%3A4599%3C781%3ANRSEIA%3E2.0.CO%3B2-F>

²² **Decadal Trends in the North Atlantic Oscillation: Regional Temperatures and Precipitation**

James W. Hurrell

Science, New Series, Vol. 269, No. 5224. (Aug. 4, 1995), pp. 676-679.

Stable URL:

<http://links.jstor.org/sici?sici=0036-8075%2819950804%293%3A269%3A5224%3C676%3ADTITNA%3E2.0.CO%3B2-L>